SINET: Ethiop. J. Sci., 47(1): 44-57, 2024 ISSN: 0379–2897 (PRINT)
 eISSN: 2520–7997

Date received: -October 2023-; Date revised: -May 2024-; Date accepted: -August 2024
DOI: https://dx.doi.org/10.4314/sinet.v47i1.4

Effects of Interfacial Layer on the Enhancement Factor of Spheroidal Metal/Dielectric Nanocomposites in Passive and Active Host Matrix

Tolasa Tamasgen Hirpha[1] and Belayneh Mesfin Ali [2,*]

[1] Department of Physics, Bonga University, P.O. Box: 334, Bonga, Ethiopia
[2] Department of Physics, Addis Ababa University, P.O. Box: 1176, Addis Ababa, Ethiopia. E-mail address: belayneh.mesfin@aau.edu.et

ABSTRACT: We investigated the effects of depolarization factor (L) and metal fraction (p) on the local field enhancement factor (LFEF) of spheroidal metal/dielectric nanocomposites (NCs) with passive and active host matrix. The expressions of the electric potentials are obtained by solving Laplace's equations in the quasistatic limit for spheroidal metal/dielectric NCs. The equation of LFEF in the host of spheroidal metal/dielectric NCs was then constructed by incorporating L and the Drude-Sommerfeld model into these formulas. The results show that, regardless of how each parameter changes or remains constant, the LFEF of the NCs has a single set of peaks in both the passive and active host matrix. The parameter L affects the LFEF curves, and the output peaks in both host media exhibit shifted symmetrical patterns. On the other hand, the media with interfacial layer (I) were significantly impacted when a field was applied to the metal/dielectric NCs medium, and the LFEF increased successively in the given frequency range with a single peak. Furthermore, in passive and active dielectric host media, the LFEF of the spheroidal shell of the NCs increased progressively with thickness. The LFEF peaks are significantly impacted by radius that was studied in both passive and active host media. We investigated that when p increases, the peak values of the LFEF in the shell structure rise. Additionally, by altering each parameter, it was possible to create an adjustable LFEF that could be utilized for optical detection, nonlinear optics, and optical sensing applications.

Keywords/ Phrases: active dielectric, enhancement factor, interfacial layer, passive dielectric host medium

INTRODUCTION

Recent developments in nanocomposites (NCs), and nanotechnology have made it possible to create reliable, extremely sensitive, and focused detection techniques that are intended to overcome some shortcomings in traditional detection systems (Caro et al., 2010). Within this context, remarkable optical phenomena that are revealed by light's interaction with NCs of spheroidal metal/dielectric NPs can create unique optical capabilities. As a result, the optical characteristics of NPs have been well investigated throughout the past century, and metal/dielectric NPs have found a number of applications in the development of next-generation ultrafast communications, signal processing systems, photonics, chemical sensing, and microelectronic devices (Genov et al., 2004). Surface plasmon resonance (SPR) controls the optical characteristics of metal probing with thin dielectric nanoparticles at interfaces, enhanced the evanescent field and heated regions emerging on the particle's surface (Maier & Atwater, 2005, Ekgasit, et al. 2004, Kooyman, 2008). The NCs of metal/dielectric NPs consist of one and two layers, i.e., the surface layer and the shell layer (Fazeli, Florez, & Simão, 2019). Hence, a unique

*Author to whom correspondence should be addressed.

structure with distinct qualities is produced by the combination of various constituent materials in NCs material, leading to a distinct structure. Consequently, NPs may include a single nanomaterial or perhaps consist of a combination of many materials (Khan, Saeed, & Khan, 2019). The dielectric function of host mediums' can be separately considered as passive and active. The active layer of the medium is more favorable because the field that passes through it increases light absorption without affecting charge transport to the electrodes (Fahendri, et al., 2022). Therefore, it is desirable to research and comprehend the properties of their enhancing field in order to construct nanoscale optical devices for real-world applications.

In order to deal with it, the local field enhancement factor (LFEF) was thoroughly experimentally and theoretically researched by many scholars (Maier & Atwater, 2005, Dynich, Ponyavina, & Filippov, 2009, Sau, et al. 2010, Hutter, Elliott & Mahajan, 2012, Klar et al., 1998). Applying the spheroidal model, numerical simulations and calculations are carried out to determine the local field enhancement factor. Moreover, the properties of NPs also rely on spatial distribution, size, and the types of embedding host matrix (Dynich, Ponyavina, & Filippov, 2009, Bergaga, Ali, & Debela, 2023, Wang, Hasanzadeh, & Meunier, 2020). Furthermore, the LFEF significantly depends on the shapes of the shell-covered nanoparticle, particularly the depolarization factors, metal fraction, interfacial factor, thickness, and surface dielectric function, which are separately considered (Werne, Testorf & Gibson, 2006).

To investigate the effects of shape, size, composition structure, and spatial distributions of NCs on the local field enhancement factor (LFEF), wide-ranging research has been conducted (Klar et al., 1998, Shewamare & Mal'nev, 2012, Karmakar, et al., 2010). However, much of this research focused on the LFEF of spherical or cylindrical metal/dielectric NCs (Abbo, Mal'nev, & Ismail, 2016, Toroghi & Kik, 2011). Prior studies show that the LFEF at the core of cylindrical and spherical metal/dielectric NP inclusions in the presence of applied NPs is sensitive to changes in shape, size, and others in the dielectric host matrix (Abbo, Mal'nev, & Ismail, 2016, Reyna & de Araújo, 2019). Noble metals like silver (Ag) have been utilized to explore the enhanced response and the nonlinear effects of NCs by applying electromagnetic field enhancement effects (Kauranen & Zayats, 2012). In this work, we investigated the effects of the depolarization factor (L), thickness (t), radius (r), metal fraction (p), interfacial factor (I), and surface dielectric permittivity (ε_s) medium on the local field enhancement factor (LFEF) of spheroidal metal/dielectric NCs in active and passive dielectric host mediums using silver (Ag) metal as a shell.

THEORETICAL MODEL AND METHODS

Theoretical model and calculation of NCs in the passive and active host matrix

We considered spheroidal shell nanocomposite in the passive and active host mediums using the quasistatic approximation. The dielectric function of the embedding medium was regarded as either passive or active to explore its results on LFEF. Depending on how the externally applied field affects the medium, the host medium's embedding dielectric function, ε_h, is referred to as passive or active. Hence, this embedding dielectric function can be written as $\varepsilon_h = \varepsilon_h' + i\varepsilon_h''$, where the real and imaginary parts of the host media are denoted by the variables ε_h' and ε_h'', respectively. The embedding dielectric function is passive when $\varepsilon_h' > 0$ and $\varepsilon_h'' = 0$, but an active embedding dielectric function is when $\varepsilon_h' = 0$, and $\varepsilon_h'' < 0$. In the present study, each component of the dielectric function was considered separately.

Considering the application of the Drude-Sommerfeld concept, ε_m, of the metallic shell's electric permittivity (Bergaga, Ali & Debela, 2022, Chettiar & Engheta, 2012), is given by:

$$\varepsilon_m = \varepsilon_\infty - \frac{1}{z(z+i\gamma)}, \quad (1)$$

where ε_∞ describes how confined electrons influence polarizability, $z = \omega/\omega_p$, $\gamma = \nu/\omega_p$ (ω_p and ω are the plasmon frequency of the bulk and the incident radiation frequencies, respectively), ν is the electron damping constant. Moreover, the real and imaginary parts of ε_m can be rewritten as

$$\varepsilon_m = \varepsilon_m' + i\varepsilon_m'', \quad (2)$$

where ε_m' and ε_m'' are the real and imaginary parts of the metal dielectric function.

Electric potential distribution in spheroidal shell nanocomposite in the host matrix

Enhancement factor for pure metal nanocomposite

An electromagnetic wave that is embedded in the host matrix and has the shape of a spheroidal impact metal/dielectric nanoparticles (NPs). So, let's take a look at the spheroidal metal/dielectric NCs model illustrated in Fig. 1 that consists of ε_m enclosed at the core of the host matrix, ε_h. Therefore, the given electrical potential equations (Pan, Huang & Li, 2001) are given as

$$\Phi_m = -E_h A r \cos\theta, \quad r_1 \leq r \quad (3)$$

$$\Phi_h = -E_h \left(r - \frac{B}{r^2}\right)\cos\theta, \quad r \geq 0, \quad (4)$$

where Φ_m and Φ_h are electrical potentials and host matrix, respectively.

At the boundary between the dielectric core and the metallic shell, the potentials must satisfy the following boundary conditions (Bohren & Huffman, 2008):

$$\Phi_m = \Phi_h | r = r_1, \quad (5)$$

$$D_m = D_h | r = r_1,$$

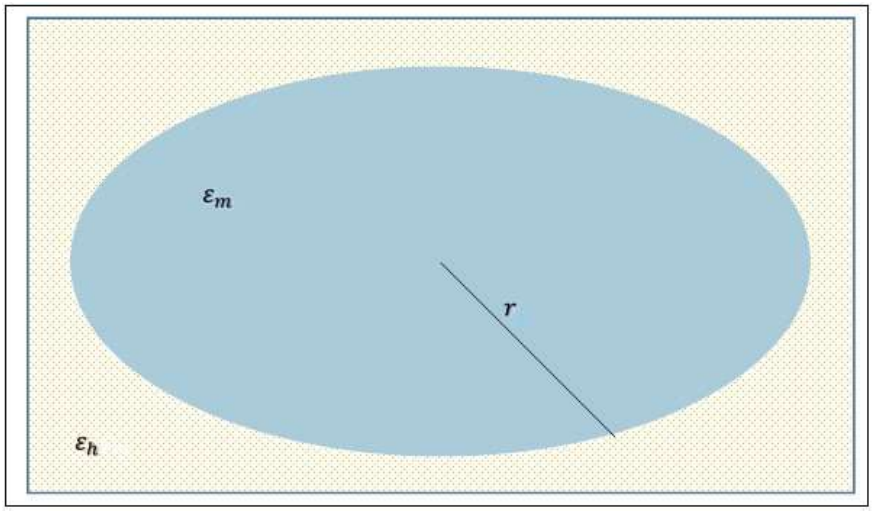

Figure 1: Schematic representation of spheroidal shell-host NCs.

Using quasistatic approaches, eqn. (3) and (4) we obtained as:

$$A = \left(1 - \frac{B}{r_1^3}\right). \quad (6)$$

Applying the displacement vector at the interface mediums using eqn. (3) and (4), and then, introducing depolarization L, we obtained:

$$L\varepsilon_m A = \varepsilon_h \left[1 + \frac{(1-L)B}{r_1^3}\right], \quad (7)$$

Therefore, the unknown coefficients A, and B of eqns. (3) and (4) expression can be summarized as follows:

$$A = \frac{\varepsilon_h}{L\varepsilon_m + \varepsilon_h(1-L)}, \quad (8)$$

$$B = \left[\frac{L(\varepsilon_m - \varepsilon_h)}{L\varepsilon_m + \varepsilon_h(1-L)}\right] \quad (9)$$

Local field enhancement factor of spheroidal of shell Nanocomposite in host matrix

To find LFEF for metal/dielectric composite of ellipsoidal nanoparticles by using the complex host matrix and eqn. (2) into eqn. (8) and squaring it we get:

$$|A|^2 = \frac{\varepsilon_h'^2 + \varepsilon_h''^2}{\left(L\varepsilon_m' + \varepsilon_h'(1-L)\right)^2 + \left(L\varepsilon_m'' + \varepsilon_h''(1-L)\right)^2}, \quad (10)$$

where

$$\varepsilon_m' = \varepsilon_\infty - \frac{1}{z^2+\gamma^2},$$

$$\varepsilon_m'' = \frac{\gamma}{z(z^2+\gamma^2)}.$$

Equation (10) is called local field enhancement factor of spheroidal metal/dielectric NPs in passive and active host matrix.

The electric potential distribution of spheroidal shell NCs with interfacial layers

Enhancement factor of pure metal nanocomposite with interfacial layer

Once more, in this section, we take into account a spheroidal metal/dielectric NPs system, as illustrated in Fig. 2, which includes a metal as a shell, ε_m, the embedding permittivity of a dielectric as a host matrix, ε_h, and finally, the interface layer between the two media, ε_s.

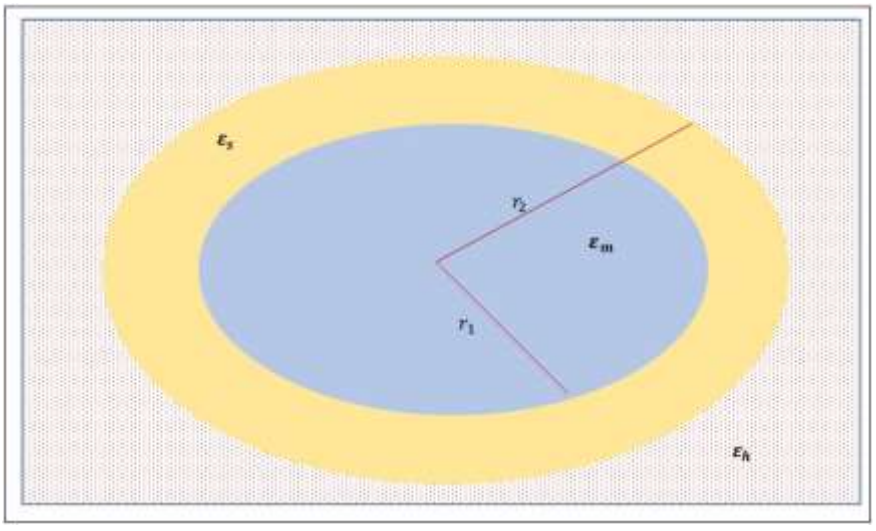

Figure 2: Schematic representation of spheroidal core-interfacial-host NCs.

The distribution of the electric potential in the system is described by the following expressions

$$\Phi_m = -E_h A r\cos\theta\,,\ r \le r_1,$$
(11)

$$\Phi_s = -E_h\left(Br - \frac{C}{r^2}\right)\cos\theta,\ \ r_1 < r \le r_1 + t,$$
(12)

$$\Phi_h = -E_h\left(r - \frac{D}{r^2}\right)\cos\theta,\ \ r > r_1 + t,$$
(13)

where Φ_m, Φ_s and Φ_h is metal dielectric, dielectric interfacial layer, and host medium electric potential function respectively.

By using the condition given in eqn. (5), and from eqns. (11) and (12) we get

$$A = B - \frac{C}{r_1^3}.$$
(14)

And also considering eqn. (5) for the displacement vector at boundary using eqn. (11) and (12), and introducing depolarization factor, we obtain

$$L\varepsilon_m A = \varepsilon_s\left[LB + \frac{(1-L)C}{r_1^3}\right].$$
(15)

Again, equating Φ_s and Φ_h, given in eqn. (13), and (14) simplifying we find:

$$B - \frac{C}{(r_1+t)^3} = 1 - \frac{D}{(r_1+t)^3}.$$
(16)

Using the definition of displacement vector at boundary condition given in eqn. (5), and applying depolarization factor, we get:

$$\varepsilon_s\left[LB + (1-L)\frac{C}{(r_1+t)^3}\right] = \varepsilon_h\left[L + (1-L)\frac{D}{(r_1+t)^3}\right]$$
. (17)

Hence, by rearranging and simplifying the expressions for the unknown coefficients A, B, C, and D of eqns. (11 - 13), we get:

$$A = \frac{\varepsilon_h\varepsilon_s}{Lb + a\varepsilon_h(1-L)},$$
(18)

$$B = \frac{\varepsilon_h(L\varepsilon_m + \varepsilon_s) + \varepsilon_s(1-L)}{Lb + a\varepsilon_h(1-L)},$$
(19)

$$C = \frac{L\varepsilon_h(\varepsilon_m - \varepsilon_s)}{Lb + a\varepsilon_h(1-L)} r_1^3,$$
(20)

$$D = \frac{b - a\varepsilon_h L}{Lb + a\varepsilon_h(1-L)}(r_1 + t)^3,$$
(21)

where

$a = L\varepsilon_m(1-p) + \varepsilon_s(1 - L + Lp)$, and

$b = \varepsilon_m(p + Lp) + L\varepsilon_m\varepsilon_s + p\varepsilon_s(1-L) + \varepsilon_s^2(1-L)$

Local field enhancement factor of spheroidal in nanocomposite with interfacial layer

Since we are using the quasistatic approach, the electric field E_h (assumed to be directed along the z-axis) is uniform. Then, by using the relation $E = -\nabla\Phi$ the local field in the metal dielectric and interfacial layer at ε_s of the spheroidal nanocomposite can be written as (Jule, et al., 2015)

$$E_s = AE_s,$$
(22)

where A is the complex function given by eqn. (22).

Now, the enhancement factor for metal/dielectric composite of spheroidal obtained at the interface mediums of the interfacial layer can be obtained by substituting the values of a and b we acquired

$$A = \frac{\varepsilon_h\varepsilon_s}{\varepsilon_m a_1 + \varepsilon_m a_2\varepsilon_h + a_3\varepsilon_h + a_4},$$
(23)

where

$a_1 = L(p + L\varepsilon_s)$, $\quad a_2 = L[1 - L - p(1-L)]$,
$a_3 = \varepsilon_s[1 - 2L + Lp(1-L) + L^2]$,

and

$a_4 = \varepsilon_s L[Lp + \varepsilon_s(1-L)]$.

where $\varepsilon_s = \frac{I}{3t}$, and , $p = 1 - \left(\frac{r_1}{r_2}\right)^3$.

By substituting the complex embedding mediums and eqn. (3) into eqn. (23), and then, squaring and simplifying it, we find the LFEF of dielectric host mediums. Finally, squaring eqn. (23) we get the LFEF equation as:

$$|A|^2 = \frac{\left(\varepsilon_h'^2 + \varepsilon_h''^2\right)\varepsilon_3^2}{\left(a_1\varepsilon_m' + a_2\varepsilon_m'\varepsilon_h' - a_2\varepsilon_m''\varepsilon_h'' + a_3\varepsilon_h' + a_4\right)^2 + \left(a_1\varepsilon_m'' + a_2\varepsilon_m'\varepsilon_h'' + a_2\varepsilon_m''\varepsilon_h' + a_3\varepsilon_h''\right)^2} \quad . \quad (24)$$

Equation (24) is called LFEF of spheroidal metal/dielectric NPs - interfacial layer in the passive and active host medium.

RESULTS AND DISCUSSION

We discussed how changing the parameters *L*, *p*, *I*, *t*, ε_s, and ε_h affect the LFEF of NCs with spheroidal shells and interfacial layers in host medium dielectrics. The model taken into consideration in the study is made up of a silver (Ag) shell, a dielectric embedded in metal, and an embedding host matrix that is (a) a passive medium, when $\varepsilon_h' = 2.25$ and $\varepsilon_h'' = 0$; (b) active medium, when $\varepsilon_h' = 0$ and $\varepsilon_h'' = -0.13886$.

In this section, we investigated the effects of the host and interfacial layer on the LFEF of spheroidal shell-interfacial layer NCs by varying the values *L*, *I*, *r*, *t*, *p*, and ε_s.

The effect of depolarization factor on LFEF

In this subsection, we discussed the effects of host medium dielectric function on the LFEF of spheroidal NCs when the depolarization factor is varied, while the rest of the parameters, such as interfacial factor, thickness, and radius, remained fixed in passive and active host mediums. The plots of $|A|^2$ versus z when the values of L are varied between 0.34 and 0.42, while other parameters are left unchanged, is illustrated in Figs. 3(a) and (b). The blue-shifted LFEF was observed as the value of the depolarization factor *L* is gradually increased from 0.34 to 0.42, as shown in Fig. 3(a).

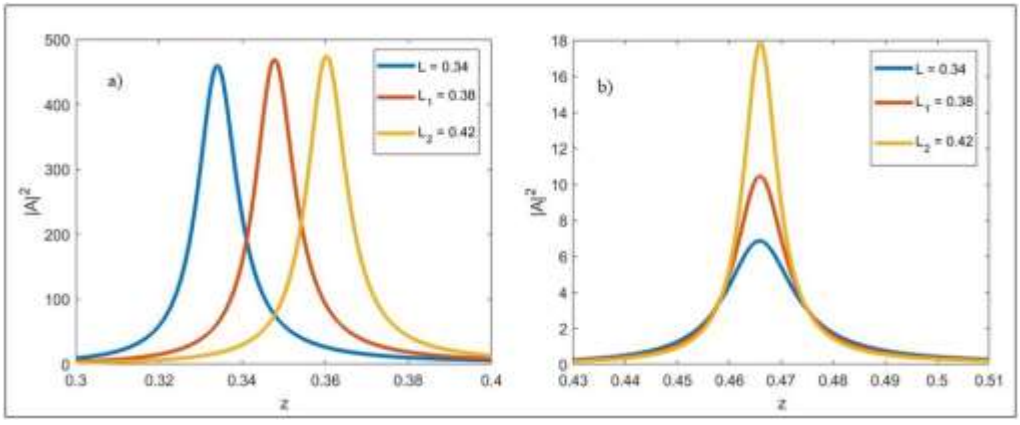

Figure 3: The effect of the depolarization factor on LFEF of spheroidal shell NCs: a) in passive dielectric shell and b) in the active dielectric shell with, $\varepsilon_h' = 2.25$, $\varepsilon_h'' = -0.13866$, $\varepsilon_\infty = 4.5$, $\omega_p = 1.45 \times 10^{16}\ rad/s$, $\gamma = 0.0115$, and different values of L.

Also, as shown in Fig. 3(b), the LFEF peaks rise with a similar upward trend as the medium becomes active. In active embedded mediums, the LFEF steadily rises for each value of L one over the other, whereas the LFEF obtained in the passive dielectric medium is blue-shifted and it is slowly increased with an increase in L values, as shown in Fig. 3(a). However, in the active embedding mediums, $\varepsilon_h'' < 0$, with a gradually increased L, the LFEF peaks are observed to increase, with no shift in position. We investigated the impacts of the depolarization factor on LFEFs as they are changed, and as can be observed in Fig. 4(a), their output peaks show no significant shifts in the passive host medium. The best position, however, is indicated by the LFEF with L_2 = 0.42, which is at z = 0.36. As a result, when an applied field impinged on the metal/dielectric nanocomposite medium, the LFEF grew progressively one after another in the specified frequency with a single peak. Additionally, we obtained symmetrical pattern peaks when the embedding host medium is decreased, for example, in passive $\varepsilon_h' = 1.30$, and $\varepsilon_h'' = 0$, while $\varepsilon_h' = 0$ and $\varepsilon_h'' = -0.13886$ for active host mediums. However, when L increased, the peaks gradually decreased, as shown in Fig. 4(a), compared with that in Fig. 3(a).

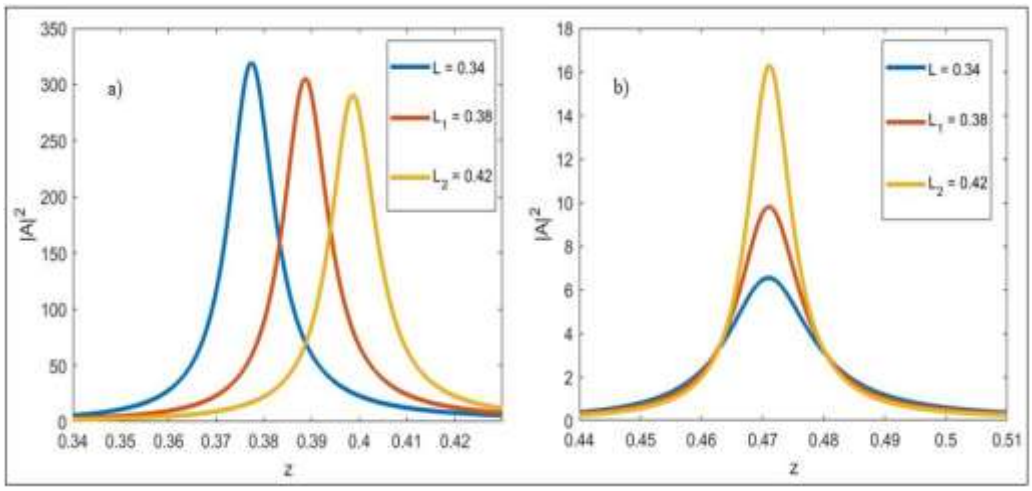

Figure 4: The effect of depolarization factor on LFEF of spheroidal shell (Ag) NCs a) in passive dielectric and b) in active dielectric host mediums with parameters: $\varepsilon_h' = 1.30$, $\varepsilon_h'' = -0.13866$, $\varepsilon_\infty = 4.5$, $\omega_p = 1.45 \times 10^{16}\, rad/s$, $\gamma = 0.0115$, **and different depolarization factor.**

Finally, we draw the conclusion that the LFEF of spheroidal metal-dielectric NPs can be influenced by the passive and active host matrix permittivity. As the dielectric function of the host medium is decreased from $\varepsilon_h' = 2.25$ to $\varepsilon_h' = 1.3$, the peaks of the LFEF is decreased significantly for a system with passive host, whereas it remains constant for a system with active host, as seen in Figs. 4(a) and (b).

The effect of depolarization factor on LFEF with interfacial layer

In this section, we investigated the LFEF of a composite of spheroidal nanoparticles made of metal/dielectric with an interfacial layer

embedded in the passive and active host matrix. By changing the depolarization factor while keeping constant the other variables, the LFEF under investigation is simulated in this case.

According to the model (Fig. 2), the interfacial medium is the space between the metal-dielectric and the spheroidal host matrix medium NCs. As a result, Figs. 5(a) and (b) illustrate the impact of depolarization factor on the effects of LFEF. The LFEF in the passive host medium is blue-shifted as the L is raised. Although the LFEF's active embedding medium is shown in Fig. 5(b).

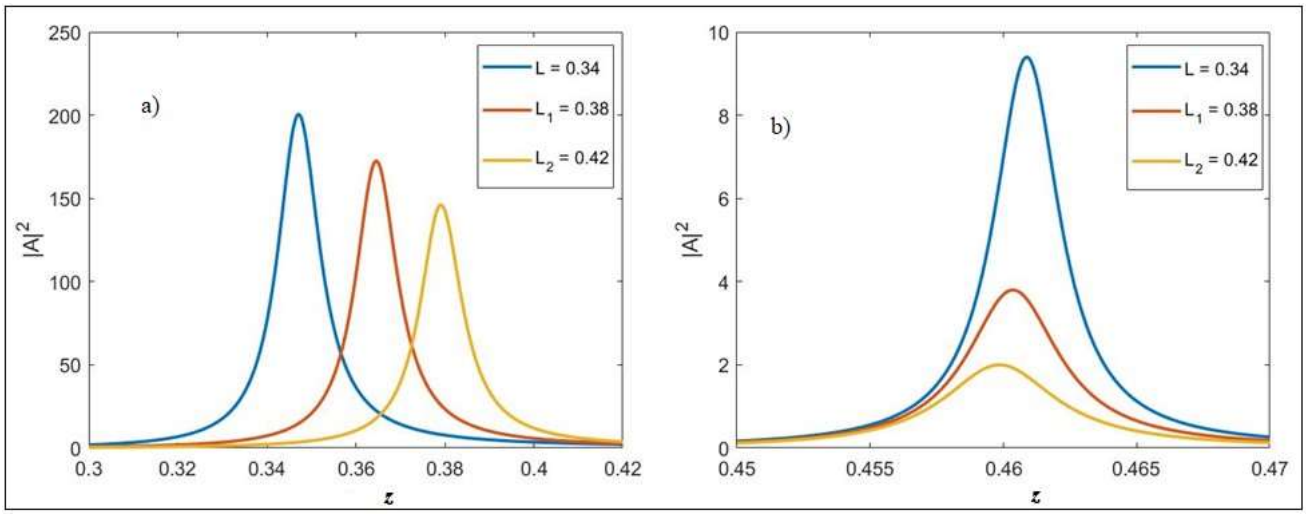

Figure 5: The Effect of depolarization factor on LFEF of spheroidal shell (Ag) NCs a) in passive dielectric and b) in active dielectric host mediums with interfacial layer parameters: $\omega_p = 1.45 \times 10^{16}\, rad/s$, $\varepsilon_\infty = 4.5$, $\gamma = 0.0115$, ***I*** **= 1.8,** r_1 **= 1.25,** ***t*** **= 0.75, and different depolarization factor.**

We also analyze the impact of the interfacial layer, *I*, via the limit where the interfacial factor, or $t \to 0$, is laid on the surface of two medium interfaces. Due to the medium's tendency to have zero thickness, this parameter may also have an impact on the LFEF of a spheroidal shell. According to eqn. (24), the only meaningful quantity is $t\varepsilon_s$. Here, the I is given to explain passing of fields using the following equation:

$$I = \lim_{\substack{t\to 0,\\ \varepsilon_s\to\infty}} t\varepsilon_s. \quad (25)$$

From eqn. (25), when t approaches 0, then $I = 0$, and in the normal condition of the electric displacement at the interface there is no jump between metallic and host dielectric functions; whereas, for an imperfect interface denoted by $I \neq 0$, the electric displacement passes across the interface mediums. Hence, managing the space of mediums between metallic and host dielectric function, *I* accordingly help to obtain the LFEF of spheroidal NPs.

We studied the effects of *L* at the interfaces between metal-like, passive, and active host matrices, by keeping parameters constant: where *I* is 1.8, *t* is 0.75, and r_1 is 1.25, the LFEF peaks are reduced. Hence, in constant thickness, interfacial factor, and radius of the interfaces as the depolarization factor increased,

the LFEF peaks decreases slowly as shown in Fig. 5(a). However, the active host medium of the interfaces can have less LFEF as seen from its output results. Also, the peaks of the active host medium decreased as the parameters like *I*, *t*, *r*, and *L* is increased.

Effect of interfacial factor on the LFEF

Next, we looked at how interfacial layer, I, affected the LFEF while the other parameters remained constant. Using the parameters I = 2.25, I_1 = 2.5, and I_2 = 2.75, the LFEF increased in the provided interfacial layer, as it is observed in Figs. 6(a) and (b). According to these findings, the interfacial layer was one of the elements that contributed to the LFEF rising as the interfacial magnitude at the interface rose. As it is seen in Figs. 6(a) and (b), it is considerably higher in passive host mediums compared to active host mediums. This demonstrated how crucial it is to have a close-fitting interfacial layer between the mediums, such as the active host matrix in a metal/dielectric nanocomposite, in order to achieve high LFEF at a specific frequency.

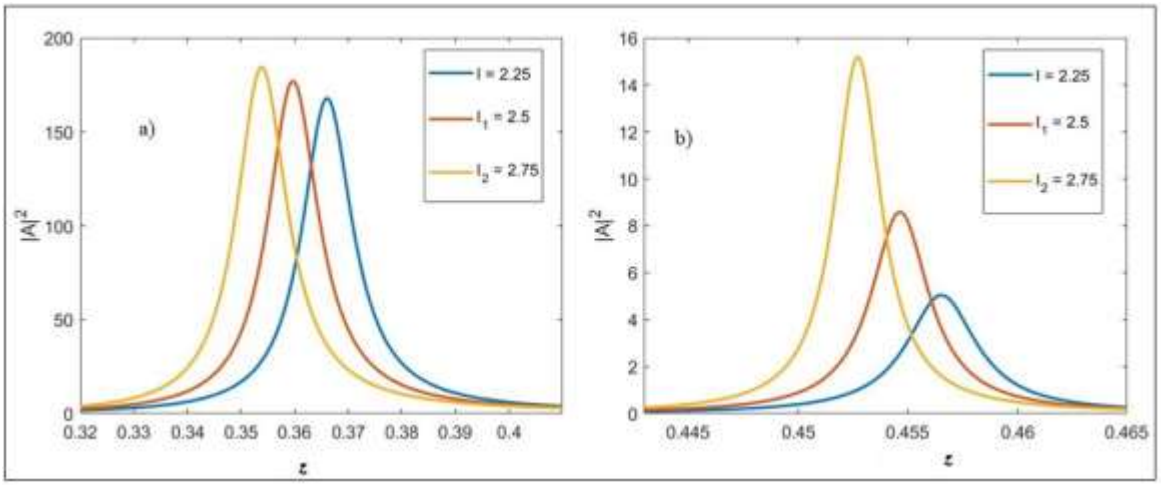

Figure 6: The effect of interfacial on LFEF of spheroidal shell NCs in a) passive and b) active host medium: ε_∞ = 4.5, *L* = 0.42, *t* = 0.75, r_1 = 1.25, $\omega_p = 1.45 \times 10^{16}\, rad/s, \gamma = 0.0115$, and different interfacial factor, *I*.

Generally, for the fixed values of L, t, and r, we are able to get a higher output of LFEF in passive medium, while less output value in active embedding media as shown in Figs. 6(a) and (b), respectively. Also, the parameters present in ε_s of NCs in passive and active host media can also affect the LFEF. Therefore, as I is increased, the peaks of the LFEF also increases and red-shifted. This is in agreement with that reported by Wu (Wu, W., et al., 2015).

Effect of thickness on LFEF of NCs

Here, we are able to create a slowly growing LFEF by adjusting the thickness of spheroidal metal/dielectric NCs, t, by fixing the following parameters constant: L = 0.36, I = 1.8, and r_1 = 1.25, as shown in Figs. 7(a) and (b). When the depolarization factor, thickness, interfacial layer, and radius were used, the effects of thickness on the LFEF were clearly investigated as shown Fig. 7. However, when the medium's thickness were raised in both passive and active dielectric host mediums, the LFEF peaks are found to increase.

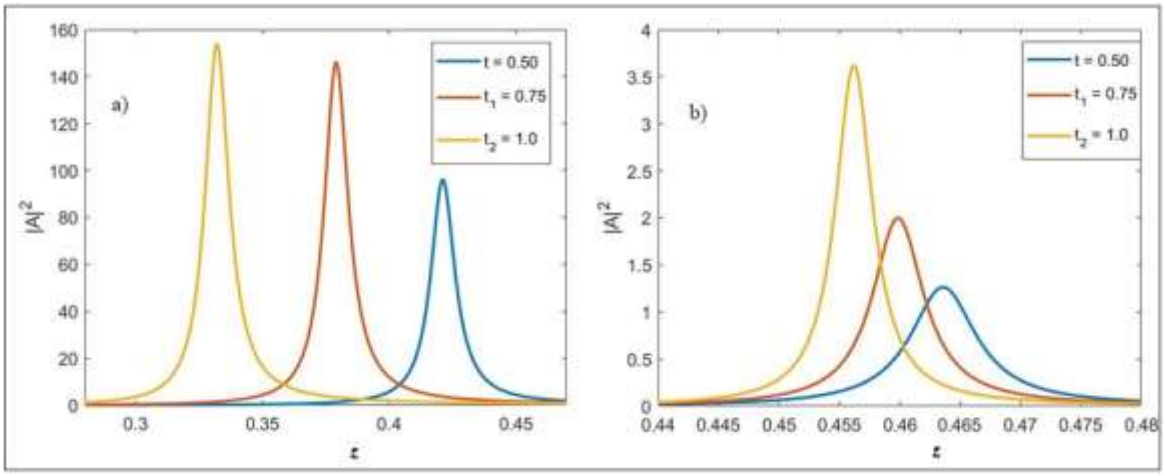

Figure 7: The effect of thickness on LFEF of spheroidal shell NCs in a) passive and b) active host medium: L = 0.42, I = 1.8, r_1 = 1.25, $\omega_p = 1.45 \times 10^{16}\ rad/s, \varepsilon_\infty = 4.5, \gamma = 0.0115$, and different thickness.

Further, as the thickness increase, the LFEF of the NCs' spheroidal shell in passive and active dielectric host mediums gradually moves to the left, as seen in Fig. 7. In the LFEF in passive host media, there are noticeable small LFEF peaks in thin thickness at the interface mediums. However, as the thickness is varied, the LFEF in the active host medium likewise shows a red-shift and increased symmetrically as thickness increased as shown in Fig. 7(b). As a result, in passive embedding host mediums, the enhancement factor with high thickness has a high peak, while in perturbed host mediums, it slowly decreases.

Likewise, in both passive and active embedding mediums the LFEFs can be affected by varying the thickness of the spheroidal metal/dielectric composite with the interfacial layer and red-shifted in both passive and active host matrix. As shown in both Figs. 7(a) and (b), changing the numerical values of the thickness in the medium may result in distinct LFEF outcomes.

Effect of radius on the LFEF of NCs

In this section, we investigated the effects of radius, r_1, on the LFEF of spheroidal metal/dielectric NPs, by fixing all the other parameters. As shown in both Figs. 8(a) and (b), the effect of radius on spheroidal NCs in passive and active host mediums greatly influenced the LFEF. However, the peaks of the LFEF are almost constant but blue-shifted as the radius increases in NCs with passive embedding materials as shown in Fig. 8(a). In contrast, the effects of radius on the LFEF is varied as the radius is increased in NCs with active medium; its peaks increases sequentially and slightly red-shifted, as shown in Fig. 8(b). Therefore, as shown in Figs. 8(a) and (b), the radius in spheroidal metal/dielectric NPs has an impact on the LFEF of spheroidal NCs. As illustrated in Fig. 8(a), increasing the radius can raise the LFEF, which is a peak that occurs at the metal/dielectric interface.

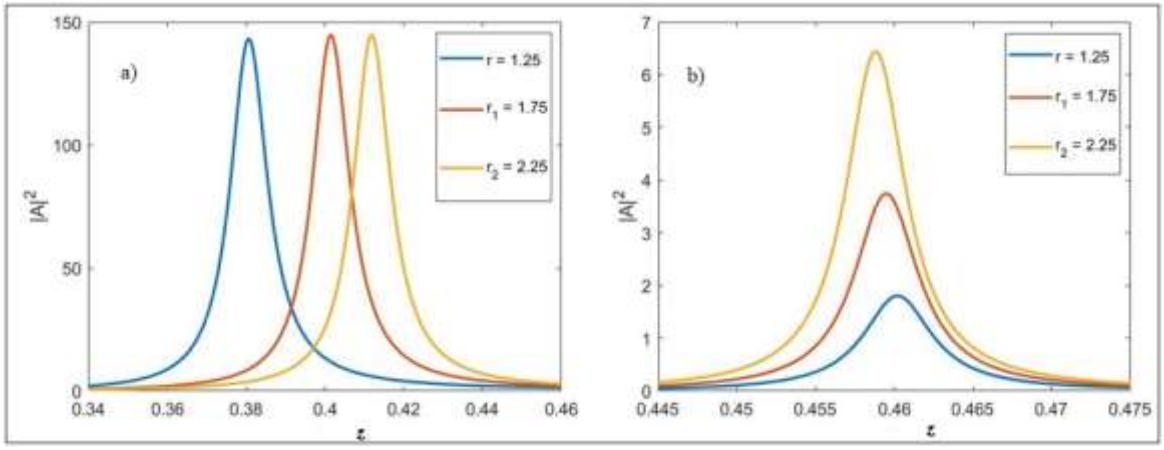

Figure 8: The effect of thickness on LFEF of spheroidal shell NCs in a) passive and b) active host medium: $\omega_p = 1.45 \times 10^{16}\ rad/s, \varepsilon_\infty = 4.5, \gamma = 0.0115$, ***L* = 0.42, *I* = 1.75, *t* = 0.75, and different radii.**

In general, when the incident field is applied to spheroidal metal-dielectric NPs in passive and active host matrix mediums, the field moves slowly in a thick medium and swiftly in a thin one. This can show us that the output result of the enhancement factor reduces, and applied fields can pass through the composite medium more easily in less dense mediums. Therefore, in order to achieve the LFEF results, we must control the parameters in the spheroidal metal/dielectric NCs with passive and active host mediums such as the parameters L, I, t, and, r_1 employed in the spheroidal shell.

The effect of metal fraction on LFEF with interfacial layer

Next, keeping the remaining parameters constant, we examined how the metal proportion affected the LFEF of spheroidal metal/dielectric NPs. We calculated the LFEF of spheroidal metal-dielectric NPs embedded in passive and active host matrix using different values of p = 0.85, 0.92, 0.99, while L = 0.36, I = 2.75, t = 0.75, and r_1 = 1.25 can affect it. This illustrates that due to the incident electromagnetic, the output intensities of the peaks of the LFEF slightly decreases as the metal fraction increases in the passive embedding medium accompanied with a red-shift, as shown in Fig. 9(a). In the NCs with active medium, the LFEF peaks increases and is blue-shifted as the metal fraction increases, as shown in Fig. 9(b).

Furthermore, as shown in Fig. 9(b), the peak values of the LFEF in the NCs increase with an increase in the metal content when the dielectric host medium becomes active and is perturbed by an incident field. The peak values, however, have a tendency to decline as the metal proportion rises in NCs with passive dielectric (Fig. 9(a)). Thus, we can see that the metal content in an active dielectric host medium has a significant impact on the LFEF of spheroidal shell NPs and causes a rise in its value.

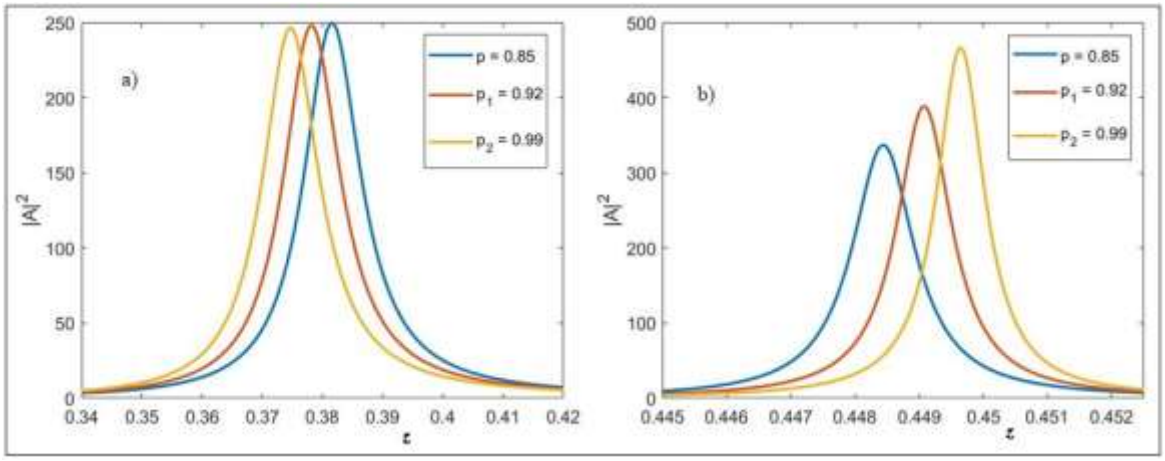

Figure 9: The effect of metal fraction on LFEF of spheroidal shell (Ag) NCs a) in passive dielectric and b) in active dielectric host mediums with parameters: $\omega_p = 1.45 \times 10^{16}\ rad/s, \varepsilon_\infty = 4.5, \gamma = 0.0115$, **$L$ = 0.36, I = 2.75, t = 0.75, r_1 = 1.25, and different values of metal fraction.**

Additionally, the peaks of the LFEF in NCs with active host medium is almost double compared to that in NCs with passive host matrix, as shown in Figs. 9(a) and (b). In both the passive and active dielectric host matrices, just one peak is visible. In general, the computational results demonstrate that the effects of metal fraction on the local field enhancement factor of spheroidal metal/dielectric NC inclusions can be significantly influenced, as shown in Fig. 9, and both of them displayed a single peak.

CONCLUSIONS

We studied the effect of passive and active permittivity of host matrix on the LFEF of spheroidal metal/dielectric NCs by varying L, p, I, t, and r. The findings demonstrate that in both passive and active host matrices, a single set of peaks is observed in the LFEF of the spheroidal metal/dielectric NCs with passive and active host matrices, regardless of how much L, p, I, and t vary or are kept constant. Furthermore, as the depolarization factor increases, the peaks seen in spheroidal metal/dielectric with passive and active host matrix gradually become less prominent. This demonstrates that when greater output values and a single LFEF peak is required, the spheroidal metal/dielectric NCs with passive host dielectric function is preferred to the active one. Additionally, we discovered that in the passive host matrix, the LFEF peaks are reduced and blue-shifted as L grows, while they decreased in the active host dielectric matrix. The peaks of LFEF are raised, and the blue shift is observed in both the passive and active host matrix as L grows. Moreover, the initial set of LFEF's peaks has red-shifted intensities as t in the passive host matrix increases. But as I grew above t, high intensities were observed, suggesting that altering the interface mediums of the geometry of spheroidal metal/dielectric NCs has a greater impact on raising the LFEF than altering the thickness of the medium at the interface.

Additionally, while the host matrix is passive, a rise in r_1 causes the LFEF's intensity to slightly increase, whereas the LFEF's intensity increases when the core is active. Furthermore, the examined LFEF peaks are both blue-shifted in the spheroidal NCs with passive host matrix, when r_1 increases while holding L, I, t, and p constant; in contrast, they are prominent in the active host matrix. Also, we discovered that by adjusting the metal fraction that is blue-shifted

in the active host matrix and red-shifted in the passive host matrix, the LFEF of the spheroidal metal/dielectric NCs may be modified. Moreover, the intensity of this peak varies significantly when its host matrix is active rather than passive. Hence, by changing these parameters and types of dielectric cores, adjustable LFEF of spheroidal metal/dielectric NCs could be obtained and used for applications in optical detection and imaging, nonlinear optics, and optical sensing.

BIBLIOGRAPHY

1. Abbo, Y. A., Mal'nev, V. N., & Ismail, A. A. (2016). Local field enhancement at the core of cylindrical nanoinclusions embedded in a linear dielectric host matrix. *arXiv preprint arXiv:1609.04700*.
2. Bergaga, G. D., Ali, B. M., & Debela, T. S. (2022). Size dependent local field enhancement factor of CdSe based core@shell spherical nanoparticles. *Materials Research Express*, *9*(4), 045001.
3. Bergaga, G. D., Ali, B. M., & Debela, T. S. (2023). Effects of shape on the optical properties of CdSe@Au core-shell nanocomposites. *AIP Advances*, *13*(3).
4. Bohren, C. F., & Huffman, D. R. (2008). Absorption and scattering of light by small particles. John Wiley & Sons.
5. Caro, C., Castillo, P. M., Klippstein, R., Pozo, D., & Zaderenko, A. P. (2010). Silver nanoparticles: sensing and imaging applications. *Silver nanoparticles*, *95*, 201-224.
6.. Chettiar, U. K., & Engheta, N. (2012). Internal homogenization: Effective permittivity of a coated sphere. *Optics express*, *20*(21), 22976-22986.
7. Dynich, R. A., Ponyavina, A. N., & Filippov, V. V. (2009). Local field enhancement near spherical nanoparticles in absorbing media. *Journal of Applied Spectroscopy*, *76*, 705-710.
8. Fahendri, F., Perdana, I., Abdullah, Z., & Muldarisnur, M. (2022). Enhancement of Light Absorption in the Active Layer of Organic Solar Cells using Ag: SiO_2 Core-Shell Nanoparticles. *Journal Penelitian Pendidikan IPA*, *8*(6), 3121-3127.
9. Fazeli, M., Florez, J. P., & Simão, R. A. (2019). Improvement in adhesion of cellulose fibers to the thermoplastic starch matrix by plasma treatment modification. *Composites Part B: Engineering*, *163*, 207-216.
10. Genov, D. A., Sarychev, A. K., Shalaev, V. M., & Wei, A. (2004). Resonant field enhancements from metal nanoparticle arrays. *Nano Letters*, *4*(1), 153-158.
11. Hutter, T., Elliott, S. R., & Mahajan, S. (2012). Interaction of metallic nanoparticles with dielectric substrates: effect of optical constants. *Nanotechnology*, *24*(3), 035201.
12. Jule, L., Mal'nev, V., Mesfin, B., Senbeta, T., Dejene, F., & Rorro, K. (2015). Fano-like resonance and scattering in dielectric (core)–metal (shell) composites embedded in active host matrices. *physica status solidi (b)*, *252*(12), 2707-2713.
13. Karmakar, B., Som, T., Singh, S. P., & Nath, M. (2010). Nanometal-glass hybrid nanocomposites: synthesis, properties and applications. *Transactions of the Indian Ceramic Society*, *69*(3), 171-186.
14. Kauranen, M., & Zayats, A. V. (2012). Nonlinear plasmonics. *Nature photonics*, *6*(11), 737-748.
15. Khan, I., Saeed, K., & Khan, I. (2019). Nanoparticles: Properties, applications and toxicities. *Arabian journal of chemistry*, *12*(7), 908-931.
16. Klar, T., Perner, M., Grosse, S., Von Plessen, G., Spirkl, W., & Feldmann, J. (1998). Surface-plasmon resonances in single metallic nanoparticles. *Physical Review Letters*, *80*(19), 4249.
17. Kooyman, R. P. (2008). Physics of surface plasmon resonance. *Handbook of Surface Plasmon Resonance*, *1*.
18. Maier, S. A., & Atwater, H. A. (2005). Plasmonics: Localization and guiding of electromagnetic energy in metal/dielectric structures. *Journal of applied physics*, *98*(1).
19. Pan, T., Huang, J. P., & Li, Z. Y. (2001). Optical bistability in metal/dielectric composite with interfacial layer. *Physica B: Condensed Matter*, *301*(3-4), 190-195.
20. Reyna, A. S., & de Araújo, C. B. (2019). High-Order Nonlinearities of Metal-Dielectric

Nanocomposites. In *Metal Nanostructures for Photonics* (pp. 61-86). Elsevier.

21. Sau, T. K., Rogach, A. L., Jäckel, F., Klar, T. A., & Feldmann, J. (2010). Properties and applications of colloidal nonspherical noble metal nanoparticles. *Advanced Materials*, *22*(16), 1805-1825.
22. Shewamare, S., & Mal'nev, V. N. (2012). Two optical bistability domains in composites of metal nanoparticles with nonlinear dielectric core. *Physica B: Condensed Matter*, *407*(24), 4837-4842.
23. Toroghi, S., & Kik, P. G. (2011, May). Design of cascaded plasmon resonances for ultrafast nonlinear optical switching. In *Enabling Photonics Technologies for Defense, Security, and Aerospace Applications VII* (Vol. 8054, pp. 52-58). SPIE.
24. Wang, L., Hasanzadeh Kafshgari, M., & Meunier, M. (2020). Optical properties and applications of plasmonic metal nanoparticles. *Advanced Functional Materials*, *30*(51), 2005400.
25. Werne, T., Testorf, M., & Gibson, U. (2006). Local-field enhancement in metal-dielectric nanocylinders with complex cross sections. *JOSA A*, *23*(9), 2299-2306.
26. Wu, W., Yue, J., Li, D., Lin, X., Zhu, F., Yin, X. ... & Jiang, K. (2015). Interface dipole enhancement effect and enhanced Rayleigh scattering. *Nano Research*, *8*, 303-319.